Shot noise enhancement from non-equilibrium plasmons in Luttinger liquid junctions

Jaeuk U Kim[1]**, Jari M Kinaret**[2] **and Mahn-Soo Choi**[3]

[1] Department of Physics, Göteborg University, SE-41296 Gothenburg, Sweden
[2] Department of Applied Physics, Chalmers University of Technology, SE-41296 Gothenburg, Sweden
[3] Department of Physics, Korea University, Seoul 136-701, Korea

E-mail: choims@korea.ac.kr

Abstract

We consider a quantum wire double junction system with each wire segment described by a spinless Luttinger model, and study theoretically shot noise in this system in the sequential tunnelling regime. We find that the non-equilibrium plasmonic excitations in the central wire segment give rise to qualitatively different behaviour compared to the case with equilibrium plasmons. In particular, shot noise is greatly enhanced by them, and exceeds the Poisson limit. We show that the enhancement can be explained by the emergence of several current-carrying processes, and that the effect disappears if the channels effectively collapse to one because of fast plasmon relaxation processes, for example.

(Some figures in this article are in colour only in the electronic version)

1. Introduction

Shot noise (SN) in electronic devices occurs because of the discrete nature of the transported charge, and manifests itself clearly in non-equilibrium situations [1, 2]. Unlike thermal (equilibrium) noise, shot noise provides additional information of the system, which is not accessible in an average current measurement [4, 5, 3]. For this reason, shot noise has been a subject of a great number of theoretical and experimental works in recent years [6].

One of the fundamental issues of current interest has been the effect of coherence on the shot noise [7]. Somewhat contrary to intuition, it has been shown that in most cases where comparable theories are available, the semiclassical and quantum mechanical descriptions give the same result; it seems that often the shot noise is not sensitive to the quantum coherence [6]. Another important issue related to the shot noise is electron–electron correlation effects, which are the subject of the present work. Popular examples are the shot noise in a single-electron transistor (SET) in the Coulomb blockade (CB) regime [3, 8] and in superconducting tunnel

junctions [9–11]. The system of our interest in this work is a one-dimensional (1D) interacting electron gas described by the Luttinger liquid (LL) model [12]. There has been a great deal of experimental effort to demonstrate that certain low-dimensional systems (e.g., carbon nanotubes) behave as Luttinger liquids [13–15]. Shot noise in Luttinger liquids has also been the subject of many recent works. For example, the non-equilibrium shot noise of the edge states was used to measure the fractional charge of the quasiparticles of the fractional quantum Hall states [16–19].

Very recently, Braggio *et al* [20] investigated the shot noise in a double junction system embedded in a Luttinger liquid. They found some features due to the interplay between the CB, the LL behaviour, and size quantization. Apart from the peculiar *quantitative* behaviour of the shot noise at higher bias voltages, its qualitative behaviour as a function of bias voltage was similar to that in conventional SET devices. They assumed an equilibrium distribution of charge-density excitations (in the following called plasmons) in all electrodes. On the other hand, in a recent work by some of the present authors [21], plasmons in the short central electrode in the absence of environment coupling were found to exhibit a highly non-equilibrium distribution. Since shot noise is sensitive to non-equilibrium fluctuations in the system, one can expect that the non-equilibrium plasmons may affect the shot noise significantly. In this work, we show that the non-equilibrium plasmons lead to *qualitatively* different behaviour of the shot noise even at relatively low bias voltages. We also show that in the limit of fast plasmon relaxation, when the plasmon distribution reaches equilibrium between successive tunnelling events, the results by Braggio and co-workers are reproduced.

2. Model

We consider an LL/LL/LL double junction with each LL representing a segment of quantum wire. We refer to the three segments as the left (L) and right (R) leads and the dot (D), respectively. The two leads are adiabatically connected to reservoirs (contacts) and the dot (the central short wire segment) is coupled to the two leads by tunnel junctions. The L and R leads are described by semi-infinite (spinless) Luttinger models while the dot is described by a finite-size (spinless) Luttinger model [20–22]. The low-energy transport properties through the system are described by the master equation [21, 23] for the probability $P(N, \{n\}, t)$ to find N (excess) electrons and n_m plasmons at mode m on the dot at time t. The eigenstates of an isolated dot are denoted by $|N, \{n\}\rangle$. The finite length L_D of the dot leads to a discrete energy spectrum of plasmons $\{n\}$ and the zero-mode energy associated with N. The equidistant plasmon spectrum is characterized by the energy spacing $\varepsilon_p \equiv \pi \hbar v_F / L_D g$, where g is the Luttinger parameter and v_F the Fermi velocity. The zero-mode energy, characterized by the energy scale $E_C = \varepsilon_p / g$, accounts for the charging effects on the dot [22]. In accordance with the *constructive* bosonization rules [22], our description of the dot in terms of the Luttinger model is justified for lengths long enough that $\varepsilon_p(L)$ is sufficiently smaller than the Fermi energy E_F of the quantum wire and the linearization of the dispersion is valid. Our bosonization also assumes short-range interaction and is valid for lengths larger than the screening length. Electrons are transferred between different wire segments by tunnelling, and the transition rates $\Gamma_{L/R}(N \pm 1, \{n'\}; N, \{n\})$ between states $|N, \{n\}\rangle$ caused by tunnelling across the two junctions are obtained using the Fermi golden rule [21]. Following the notations of [21], we consider that the LL-parameter g is the same for each wire segment; the capacitances across L/R tunnelling junctions are taken to be the same ($C_L = C_R$), but the tunnelling amplitudes may differ and their ratio is denoted by $R = |t_L|^2 / |t_R|^2$. The explicit form of the transition rates for a wire with a single branch of spinless fermions at applied voltage $V = V_L - V_R$ is

given by [21]

$$\Gamma_{\text{L/R}}(N, \{n\} \to N', \{n'\}) = 2\pi |t_{\text{L/R}}|^2 / \hbar \gamma (E_{\text{D}}(N', \{n'\}) - E_{\text{D}}(N, \{n\}) \mp (N' - N)eV_{\text{L/R}})$$
$$\times |\langle N', \{n'\} | \psi_{\text{D}}^{\dagger} \delta_{N', N+1} + \psi_{\text{D}} \delta_{N', N-1} | N, \{n\} \rangle|^2, \tag{1}$$

where the contribution of the leads is

$$\gamma(\epsilon) = \frac{1}{2\pi\hbar} \frac{1}{\pi v_{\text{F}}} \left(\frac{2\pi \Lambda_g}{\hbar v_{\text{F}} \beta} \right)^{\alpha} \left| \Gamma\left(\frac{\alpha+1}{2} + i\frac{\beta\epsilon}{2\pi} \right) \right|^2 \frac{e^{-\beta\epsilon/2}}{\Gamma(\alpha+1)} \tag{2}$$

and the contribution of overlap matrix elements in the central segment is

$$|\langle\{n'\}|\psi_{\text{D}}^{\dagger}|\{n\}\rangle|^2 = \frac{1}{L_{\text{D}}} \left(\frac{\pi\Lambda}{L_{\text{D}}} \right)^{\alpha} \prod_{m=1}^{\infty} \left(\frac{1}{mg} \right)^{|n'_m - n_m|} \frac{n_m^{(<)}!}{n_m^{(>)}!} \left[L_{n_m^{(<)}}^{|n'_m - n_m|} \left(\frac{1}{mg} \right) \right]^2 \tag{3}$$

where $n_m^{(<)} = \min(n'_m, n_m)$ and $n_m^{(>)} = \max(n'_m, n_m)$. Here $L_m^n(z)$ is a Laguerre polynomial, Λ a short-distance cutoff, and $\alpha = (g^{-1} - 1)$ the appropriate exponent for tunnelling into the end of a Luttinger liquid. Note that while the lead contribution depends only on the energies E_{D} of the involved states of the dot, the contribution arising from the dot depends on the detailed nature of the participating states. Temperature enters the rates through $\beta = 1/(k_{\text{B}}T)$; since we are interested in shot noise rather than thermal noise, we from now on set $k_{\text{B}}T$ to a value far below any relevant energy scale in the dot.

The plasmons in the two leads, being in contact with reservoirs with many low-energy excitations, are assumed to be in equilibria separately. However, the plasmons in the dot are driven far from the equilibrium distribution [21] by tunnelling electrons. This deviation is already significant at relatively low bias voltages $2\varepsilon_{\text{p}} \leqslant eV \leqslant 2E_{\text{C}}$. In contrast to the equilibrium plasmons [20] that produce qualitatively similar shot noise as in a usual SET [3], the non-equilibrium distribution strongly affects the SN of the system.

The coupling of the system to the environment causes even the plasmon distribution in the dot to relax towards an equilibrium. The precise form of the relaxation rate, Γ_{p}, depends on the specific relaxation mechanism, but the physical properties of our concern are not sensitive to such details. We use a phenomenological model, obeying detailed balance, with

$$\Gamma_{\text{p}}(\{n'\}, \{n\}) = \gamma_{\text{p}} \frac{W_{\text{p}}/\varepsilon_{\text{p}}}{e^{\beta W_{\text{p}}} - 1} \tag{4}$$

where $W_{\text{p}} = \varepsilon_{\text{p}} \sum_m m(n'_m - n_m)$ is the energy difference of the two many-body states with $\{n'\}$ and $\{n\} = (n_1, n_2, \ldots, n_m, \ldots)$ plasmon occupations, and $\beta = 1/k_{\text{B}}T$ is the inverse temperature. While the plasmon relaxation rate in nanoscale structures is difficult to estimate, recent computer simulations on carbon nanotubes indicate that plasmon excitations in them have lifetimes of the order of a picosecond, much longer than those in three-dimensional structures [24]. The total transition rate is hence given by a sum of rates associated with tunnelling and plasmon relaxation, $\Gamma(N', \{n'\}; N, \{n\}) = \sum_{\ell=\text{L,R}} \Gamma_{\ell}(N', \{n'\}; N, \{n\}) + \delta_{N',N} \Gamma_{\text{p}}(\{n'\}, \{n\})$ where ℓ labels the tunnel junctions. The only phenomenological parameter is the timescale of the relaxation processes in the dot, γ_{p}; all other quantities are determined by the geometry of the system and the properties of the tunnel junctions.

The master equation approach neglects phase coherence of electrons tunnelling across the two junctions (sequential tunnelling regime). The effects of the coherence on the SN have been hotly debated in recent years. However, for many mesoscopic systems (including low-dimensional interacting systems), the master equation approach yields the same results as the fully quantum mechanical description of the SN [6]. Furthermore, the sequential tunnelling picture is known to provide a good approximation at temperatures above the inverse lifetime

of the dot states ($k_B T > \Gamma$). Therefore, we expect that our master equation approach yields qualitatively correct results for the system at hand, which is weakly coupled to the leads.

We introduce a matrix notation for the transition rates Γ with matrix elements defined by

$$[\hat{\Gamma}_\ell^\pm(N)]_{\{n'\},\{n\}} = \Gamma_\ell(N \pm 1, \{n'\}; N, \{n\}), \tag{5}$$

$$[\hat{\Gamma}_\ell^0(N)]_{\{n'\},\{n\}} = \delta_{\{n'\},\{n\}} \sum_{\{n''\}} [\hat{\Gamma}_\ell^+(N) + \hat{\Gamma}_\ell^-(N)]_{\{n''\},\{n\}}, \tag{6}$$

and

$$[\hat{\Gamma}_p(N)]_{\{n'\},\{n\}} = -\Gamma_p(\{n'\}, \{n\}) + \delta_{\{n'\},\{n\}} \sum_{\{n''\}} \Gamma_p(\{n''\}, \{n\}). \tag{7}$$

Using this notation, the master equation is

$$\frac{\mathrm{d}}{\mathrm{d}t} |P(t)\rangle = -\hat{\Gamma} |P(t)\rangle \tag{8}$$

with $\hat{\Gamma} = \hat{\Gamma}_p + \sum_{\ell=L,R} (\hat{\Gamma}_\ell^0 - \hat{\Gamma}_\ell^+ - \hat{\Gamma}_\ell^-)$, where $|P(t)\rangle$ is the column vector (not to be confused with the 'ket' in quantum mechanics) with elements given by $\langle N, \{n\}|P(t)\rangle \equiv P(N, \{n\}, t)$.

3. Shot noise

We investigate the shot noise power defined by

$$S(\omega) = 2 \int_{-\infty}^{\infty} \mathrm{d}\tau \, \mathrm{e}^{+i\omega\tau} [\langle I(t+\tau)I(t)\rangle - \langle I(t)\rangle^2] \tag{9}$$

in the steady state ($t \to \infty$). In terms of the *tunnelling* current $I_{L/R}$ across the junction L/R, the *total* current I is conveniently written as $I = \sum_{\ell=L,R} (C/C_\ell) I_\ell$, where $C^{-1} = C_L^{-1} + C_R^{-1}$. The correlation functions $K(\tau) = \langle I_\ell(t+\tau)I_{\ell'}(t)\rangle$ ($t \to \infty$) can be deduced from the master equation (8); in the matrix notation [3, 8] we have

$$K(\tau) = e^2 \sum_{N,\{n\}} \langle N, \{n\}| [\Theta(+\tau)\hat{I}_\ell \exp(-\hat{\Gamma}\tau)\hat{I}_{\ell'} $$
$$+ \Theta(-\tau)\hat{I}_{\ell'} \exp(+\hat{\Gamma}\tau)\hat{I}_\ell + \delta(\tau)\delta_{\ell\ell'}(\hat{\Gamma}_\ell^+ + \hat{\Gamma}_\ell^-)] |P(\infty)\rangle, \tag{10}$$

where $\Theta(x)$ is the unit step function, $|P(\infty)\rangle$ is the steady-state solution to the master equation (8), and $\hat{I}_{L/R}$ are tunnelling current matrices $\hat{I}_{L/R} = \mp e(\hat{\Gamma}_{L/R}^+ - \hat{\Gamma}_{L/R}^-)$.

For bias voltages and temperatures when only a few levels are involved in the transport, the Fano factor $F \equiv S(0)/2e\langle I \rangle$ can be evaluated analytically, but the general case requires numerical integration of equation (8). Figure 1 shows a typical behaviour of the Fano factor as a function of bias voltage for different values of the interaction parameter g. The dips at $eV = 2E_C = 2\varepsilon_p/g$ for $g = 0.7$ and $g = 0.5$ in figure 1(a) are ascribed to the charging effect as typically seen in SET devices [3, 8]. This dip structure was also observed by Braggio *et al* [20].

A remarkable feature that contrasts our model with a conventional SET [3, 8], and the model in [20], is the enhancement of the shot noise in the bias range $2\varepsilon_p < eV < 2E_C$; see figure 1(a). As the external bias voltage increases over the threshold value $2\varepsilon_p$, it provides an electron with enough energy to tunnel across the double junction through the plasmon excitation level of mode $m = 1$, and hence the current sharply increases [21, 23]. Unlike a usual resonance channel, however, this additional channel is very noisy in the sense that the Fano factor exceeds the conventional Poisson limit ($F = 1$). Therefore, the statistics of the tunnelling events across the double junction through the plasmon excitations are highly non-Poissonian.
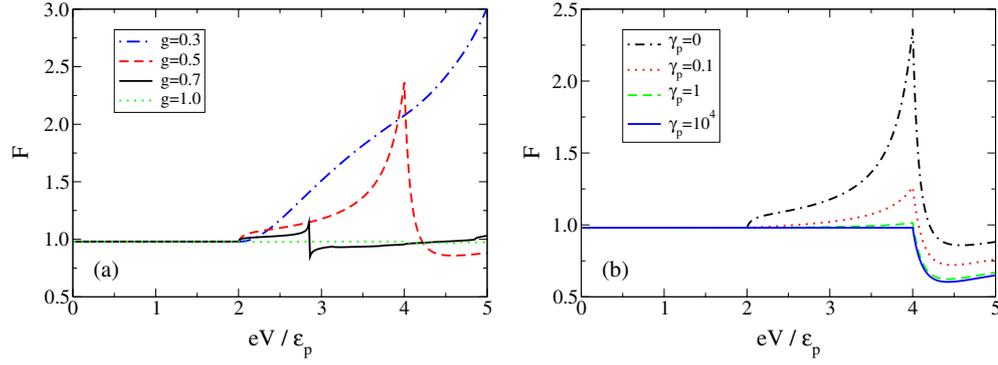
Figure 1. Fano factor $F \equiv S(0)/2e\langle I \rangle$ as a function of bias voltage (a) for $g = 0.3, 0.5, 0.7, 1$, with no plasmon relaxation on the dot, and (b) for $g = 0.5$ with different plasmon relaxation rates (γ_p). Here $R = 100$ (highly asymmetric junctions), and $T = 0$.

We emphasize that the SN enhancement is due to the non-equilibrium distribution of the plasmons on the dot. To see this, we turn on the plasmon relaxation, $\gamma_p \neq 0$. For sufficiently large relaxation rates, any plasmon excitations induced by electron tunnelling relax to an equilibrium before a subsequent tunnelling event. Therefore, as the plasmon relaxation rate increases, the Fano factor should recover the characteristic of the conventional SET or the model of Braggio *et al* [20]. This is clearly seen in figure 1(b), where the Fano factor is shown as a function of eV for relative plasmon relaxation rates $\gamma_p/\Gamma_0 = 0, 0.1, 1, 10^4$, where $\Gamma_0 = |t|^2/\hbar^2 v_F L_D$ with $|t|^{-2} = |t_L|^{-2} + |t_R|^{-2}$.

A simple explanation of the enhanced noise may be obtained by considering a situation in which only three states of the dot are energetically allowed. We denote the states $|0\rangle$, $|1A\rangle$ and $|1B\rangle$, where the integer denotes the (excess) number of charges, and A and B label different states with the same particle number[4]. The transition rates between these states, caused by tunnelling events into and out of the dot, are given by Γ_α^s, where $s = \pm$ indicates if the transition is from charge state 0 to charge state 1 or vice versa, and the label $\alpha = A, B$ tells which of the states $|1A\rangle$ and $|1B\rangle$ is involved in the transition. Hence, there are two current-carrying processes involving transitions $|0\rangle \rightarrow |1\alpha\rangle \rightarrow |0\rangle$, and, in a time sequence, the two processes alternate randomly. This extra degree of freedom results in additional noise, and is reflected in the Fano factor (which can be calculated as described above)

$$F = 1 + \frac{\Gamma_A^+ \Gamma_B^+ (\Gamma_A^- - \Gamma_B^-)^2 - \Gamma_A^- \Gamma_B^- (\Gamma_A^- \Gamma_B^+ + \Gamma_A^+ \Gamma_B^-)}{(\Gamma_A^+ \Gamma_B^- + \Gamma_A^- \Gamma_B^+ + \Gamma_A^- \Gamma_B^-)^2} \quad (11)$$

that can exceed unity if the two processes correspond to very different current levels; in the case studied above this happens when the interaction is sufficiently strong. With this consideration, it is clear that the enhanced shot noise comes from the multiplicity of available transport channels, which in our case are provided by the plasmon modes, contributing to the total current with different amplitudes. The shot noise is enhanced because of fluctuations between channels. The interpretation is consistent with similar findings in different systems [25, 26] as well. If there is a fast internal relaxation process that allows the state $|1B\rangle$ to decay to $|1A\rangle$,

---

[4] In the case studied above, this three-state model is reasonably accurate for $2\varepsilon_p \lesssim eV \ll 2E_C$, when A corresponds to the state with no plasmon excitations and B to the state with one plasmon at the mode $m = 1$ ($n_1 = 1$).
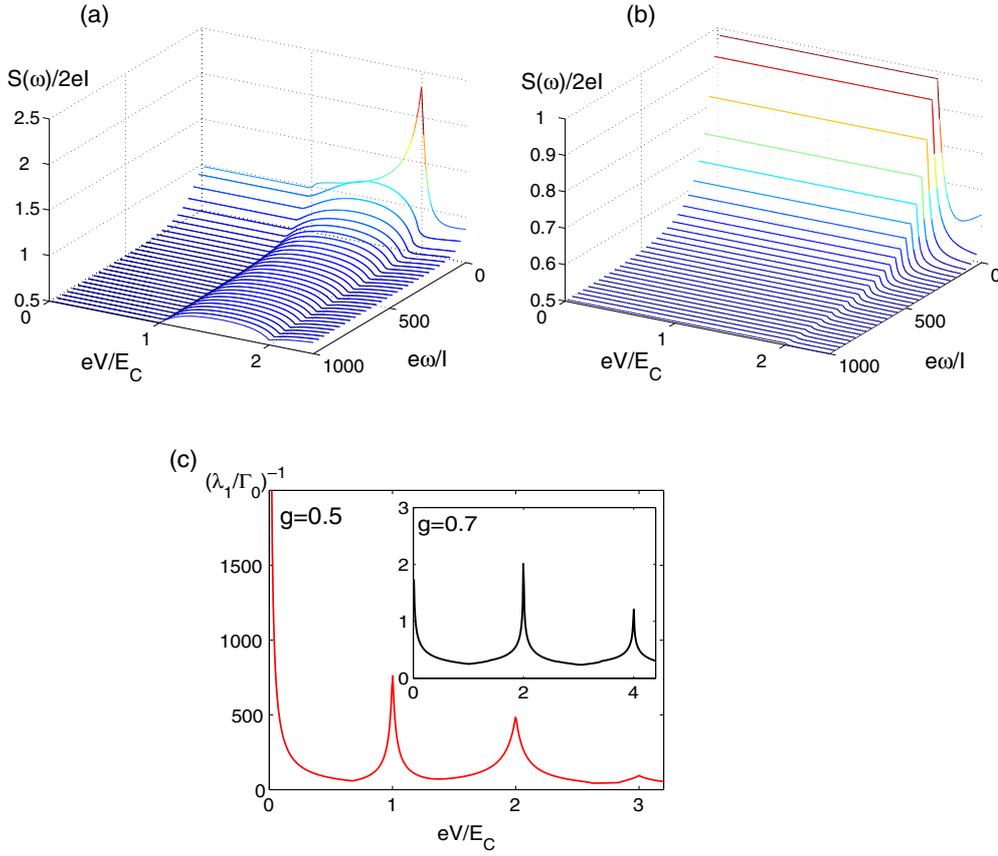
Figure 2. Finite frequency shot noise $S(\omega)/2eI$ as a function of the bias eV/E_C and frequency $e\omega/I$ for $R = 100$ and $g = 0.5$, at $N_G = 1/2$ ($T = 0$), (a) with no plasmon relaxation ($\gamma_p = 0$) and (b) with fast plasmon relaxation ($\gamma_p = 10^4$). In (c), the longest relaxation time with $\gamma_p = 0$ as a function of the applied voltage for strong and weak interactions ($g = 0.5$ and 0.7, respectively) is plotted. The relaxation time is given in units of $\Gamma_0 = |t|^2/\hbar^2 v_F L_D$ with $|t|^{-2} = |t_L|^{-2} + |t_R|^{-2}$.

the two channels effectively collapse into one, and the Fano factor is given by

$$F = \frac{[\Gamma_A^-]^2 + [\Gamma_A^+ + \Gamma_B^+]^2}{[\Gamma_A^- + \Gamma_A^+ + \Gamma_B^+]^2} \in \left[\frac{1}{2}, 1\right] \tag{12}$$

which is the result for a single channel system with transition rates $\Gamma^- = \Gamma_A^-$ and $\Gamma^+ = \Gamma_A^+ + \Gamma_B^+$. Hence, the presence of charge-conserving internal relaxation processes reduces the effective number of transport processes, and the noise associated with the random alternation between them.

The shot noise enhancement persists to quite high frequencies as shown in figure 2, where the shot noise power $S(\omega)/(2eI)$ is shown as a function of the bias and frequency for a strong interaction ($g = 1/2$) and asymmetric tunnel barriers ($R = 100$) without plasmon relaxation (a) and with fast plasmon relaxations (b).

The frequency dependence of noise reveals two additional consequences of non-equilibrium plasmons. First, the asymptotic high-frequency value of $S(\omega)$ is increased by the non-equilibrium distribution, and second, the characteristic frequency scale of the noise is seen to depend quite sensitively on the applied voltage.

In the high-frequency limit, $\omega \to \infty$, the correlation effects are lost in the noise power except the $\delta(\tau)$-term in (10) that reflects the Pauli exclusion [8], and the asymptotic value of the noise spectrum reduces to

$$S(\mathrm{i}\omega \to \infty) = 2e\left(\frac{C_{\mathrm{R}}^2 A_{\mathrm{L}}}{(C_{\mathrm{L}} + C_{\mathrm{R}})^2} + \frac{C_{\mathrm{L}}^2 A_{\mathrm{R}}}{(C_{\mathrm{L}} + C_{\mathrm{R}})^2}\right) = \frac{e}{2}(A_{\mathrm{L}} + A_{\mathrm{R}}), \tag{13}$$

where $A_{\mathrm{L/R}}$ in the steady state is given by

$$A_\ell = e \sum_{N,\{n\}} \langle N, \{n\}|\hat{\mathbf{\Gamma}}_\ell^+ + \hat{\mathbf{\Gamma}}_\ell^-|P(\infty)\rangle. \tag{14}$$

The quantity A_ℓ counts the total number of tunnelling events across the junction ℓ, without regard to direction. In the absence of tunnelling events against the voltage, which is the case for example in the limit of fast plasmon relaxation and low temperatures, the limiting value of $S(\omega)$ is simply proportional to the current. In the non-equilibrium case, however, some plasmon modes with sufficiently high energy are occupied, so tunnelling against the voltage is not negligible, which results in the enhanced high-frequency noise above the customary limiting value $S(\omega \to \infty) = eI$.

The frequency dependence of $S(\omega)$ comes from terms of the form $\lambda_j/(\omega^2 + \lambda_j^2)$ (see equation (10)), where λ_j are the non-zero eigenvalues of the transition matrix Γ, that is, the characteristic relaxation rates of the system. The longest relaxation time, shown in figure 2(c) for $g = 0.5$ and 0.7, exhibits maxima at threshold voltages when more states (either charge states or additional plasmon excitations) become involved in the transport. The long relaxation time reflects the slow transition rates to, or from, these states near the energy threshold. For strong interactions ($g = 0.5$ in the figure), clear maxima are seen both at thresholds for additional plasmon states ($eV = (2g)E_{\mathrm{C}}$) and for new charge states ($eV = 2E_{\mathrm{C}}$), while for weaker interactions, the structure at plasmon excitations is almost washed away. This is because for weak interactions, the transition rates are roughly given by step functions, in contrast to the strong interaction case when they increase like a power law with a larger exponent.

4. Conclusions

We have investigated the shot noise of a Luttinger liquid double-barrier structure. The non-equilibrium plasmons on the central segment strongly affect current fluctuations even at low bias voltages $2\varepsilon_{\mathrm{p}} \leqslant eV < 2E_{\mathrm{C}}$. The shot noise is enhanced beyond the Poissonian limit because of the emergence of competing transport processes; the enhancement is more pronounced for stronger interactions, and persists to unexpectedly high frequencies.

Acknowledgments

References

[1] Schottky W 1918 *Ann. Phys., Lpz.* **57** 541
[2] Hull A W and Williams N H 1925 *Phys. Rev.* **25** 147
[3] Hershfield S, Davies J H, Hyldgaard P, Stanton C J and Wilkins J W 1993 *Phys. Rev.* B **47** 1967

[4] Davies J H, Hyldgaard P, Hershfield S and Wilkins J W 1992 *Phys. Rev.* B **46** 9620

[5] Wilkins J W, Hershfield S, Davies J H, Hyldgaard P and Stanton C J 1992 *Phys. Scr.* T **42** 115

[6] Blanter Y M and Büttiker M 2000 *Phys. Rep.* **336** 1

[7] Oberholzer S, Sukhorukov E V and Schönenberger C 2002 *Nature* **415** 765 and references therein

[8] Korotkov A N 1994 *Phys. Rev.* B **49** 10381

[9] Deblock R, Onac E, Gurevich L and Kouwenhoven L P 2003 *Science* **301** 203

[10] Choi M S, Plastina F and Fazio R 2003 *Phys. Rev.* B **67** 045105

[11] Choi M S, Plastina F and Fazio R 2001 *Phys. Rev. Lett.* **87** 116601

[12] Haldane F D M 1981 *J. Phys. C: Solid State Phys.* **14** 2585

[13] Bockrath M, Cobden D H, Lu J, Rinzler A G, Smalley R E, Balents L and McEuen P L 1999 *Nature* **397** 598

[14] Yao Z, Postma H W C, Balents L and Dekker C 1999 *Nature* **402** 273

[15] Postma H W C, Teepen T, Yao Z, Grifoni M and Dekker C 2001 *Science* **293** 76

[16] Kane C L and Fisher M P A 1994 *Phys. Rev. Lett.* **72** 724

[17] Saminadayar L, Glattli D C, Jin Y and Etienne B 1997 *Phys. Rev. Lett.* **79** 2526

[18] de-Picciotto R, Reznikov M, Heiblum M, Umansky V, Bunin G and Mahalu D 1997 *Nature* **389** 162

[19] Comforti E, Chung Y C, Heiblum M, Umansky V and Mahalu D 2002 *Nature* **416** 515

[20] Braggio A, Fazio R and Sassetti M 2003 *Phys. Rev.* B **67** 233308

[21] Kim J U, Krive I V and Kinaret J M 2003 *Phys. Rev. Lett.* **90** 176401

[22] von Delft J and Schoeller H 1998 *Ann. Phys., Lpz.* **7** 225

[23] Braggio A, Grifoni M, Sassetti M and Napoli F 2000 *Europhys. Lett.* **50** 236

[24] Tománek D 2004 private communication

[25] Sukhorukov E V, Burkard G and Loss D 2001 *Phys. Rev.* B **63** 125315

[26] Isacsson A and Nord T 2004 *Europhys. Lett.* **66** 708